Electrochemical mineralization of sulfamethoxazole over wide pH range using FeIIFeIII LDH modified carbon felt cathode: Degradation pathway, toxicity and reusability of the modified cathode

Soliu O. Ganiyu, Thi Xuan Huong Le, Mikhael Bechelany, Nihal Oturan, Stefano Papirio, Giovanni Esposito, Eric D. van Hullebusch, Marc Cretin, Mehmet A. Oturan

Electrochemical mineralization of sulfamethoxazole over wide pH range using $Fe^{II}Fe^{III}$ LDH modified carbon felt cathode: Degradation pathway, toxicity and reusability of the modified cathode

Soliu O. Ganiyu[1], Thi Xuan Huong Le[2], Mikhael Bechelany[2,*], Nihal Oturan[1], Stefano Papirio[3], Giovanni Esposito[4], Eric van Hullebusch[5], Marc Cretin[2],Mehmet A. Oturan[1*]

[1]*Université Paris-Est, Laboratoire Géomatériaux et Environnement (LGE), EA 4508, UPEM, 77454 Marne-la-Vallée, France*

[2]*IEM (Institut Européen des Membranes), UMR 5635, CNRS, ENSCM, UM, Université de Montpellier, Place E. Bataillon, F-34095 Montpellier, Cedex 5, France*

[3]*Department of Civil, Architectural and Environmental Engineering, University of Napoli Federico II, Via Claudio 21, 80125 Napoli, Italy*

[4]*Department of Civil and Mechanical Engineering, University of Cassino and Southern Lazio, Via Di Biasio 43, 03043 Cassino (FR), Italy*

[5]*IHE Delft, Institute for Water Education, Westvest 7, 2611 AX Delft, The Netherlands*

Manuscript submitted to the Chemical Engineering Journal

* Corresponding author's emails:

mikhael.bechelany@umontpellier.fr (MikhaelBechelany)

mehmet.oturan@u-pem.fr(Mehmet A. Oturan)

Abstract

Hierarchical three-dimensional (3D) porous architecture $Fe^{II}Fe^{III}$ layered double hydroxide (LDH) multiwall was grown on carbon-felt (CF) substrate via solvothermal process. The as-deposited $Fe^{II}Fe^{III}$ LDH/CF cathode was composed of highly oriented and well crystallized interconnected nanowalls with high electrical conductivity and excellent catalytic activity over a wide pH range (pH 3 – 9) for heterogeneous electro-Fenton (HEF) degradation of antibiotic sulfamethoxazole (SMT) in aqueous medium. Mineralization efficiencies (in terms of TOC removal) of ~97%, 93% and 90% was achieved at pH 3, 6 and 9 respectively for $Fe^{II}Fe^{III}$ cathode during HEF treatment of 0.2 mM SMT solution at applied current density of 7.5 mA cm^{-2} using Ti_4O_7 anode. Comparative electro-Fenton (EF-Fe^{2+}) with 0.2 mM Fe^{2+} or electrooxidation with H_2O_2 production (EO-H_2O_2)studies using raw CF cathode at similar experimental conditions showed relatively lower mineralization with highest TOC removal efficiency of 77% and 64% obtained at pH 3 for EF-Fe^{2+} and EO-H_2O_2 respectively. Oxidative degradation of SMT in HEF system was by (i) Ti_4O_7($^{\bullet}$OH) generated at anode surface at all pH studied, (ii) surface catalyzed process and (iii) contribution from homogeneous catalyzed process at pH 3 due to leached iron ions. The prepared $Fe^{II}Fe^{III}$ LDH/CF exhibited excellent catalytic stability with good reusability up to 10 cycles of 4 h treatment at pH 6. Initial SMT solution showed relatively high toxicity but total detoxification of the solution was attained after 8 h of treatment by HEF with

$Fe^{II}Fe^{III}$LDH/CF cathode. HEF with $Fe^{II}Fe^{III}$ LDH/CF cathode is an exciting technique for remediation of organic contaminated wastewater.

Keywords: $Fe^{II}Fe^{III}$ LDH modified carbon felt, heterogeneous electro-Fenton, catalytic activity, Sulfamethoxazole, mineralization, Microtox® toxicity

1. Introduction

Nowadays, electrochemical advanced oxidation processes (EAOPs) receive increasing attention due to their excellent potential for total destruction of refractory organic pollutants in wastewater [1–4]. Although, there are still few skepticism surrounding it full implemented on industrial scale due to the lack of technology certification and limited large-scale applications, the potential of the process has received the attention of some industrial players, who are currently perfecting the engineering design and operational parameters optimization for efficient and profitable industrial scale usage [5]. These eco-friendly wastewater treatment techniques utilize on-site generated reactive oxygen species, mostly hydroxyl radicals ($^{\bullet}OH$), which is the second strongest oxidizing species after fluorine (E^o ($^{\bullet}OH/H_2O$) = 2.80 V/SHE) and can non-selectively oxidize organic pollutants until their total mineralization (electrochemical combustion) to CO_2, water and inorganic ions [6–9]. EAOPs based on Fenton's chemistry (electro-Fenton and related process) are one of the most widely studied techniques among EAOPs for wastewater treatment [2,3]. In electro-Fenton process (EF), $^{\bullet}OH$ are continuously produced *via* the reaction between electrochemically generated Fenton's reagent ($H_2O_2 + Fe^{2+}$) (eq. 1) in the bulk solution [2,3,6,8].The required H_2O_2 is continuously electrogenerated on-site by the reduction of O_2 at the cathode (eq. 2) and only small amount of Fe^{2+} is added to catalyze its decomposition,thanksto continuousFe^{2+}production from the Fe^{3+} produced in Fenton's reaction (eq.1) by electro-reduction at the cathode (eq. 3) [2,3,10].

$$Fe^{2+} + H_2O_2 + H^+ \rightarrow Fe^{3+} + H_2O + {}^{\bullet}OH \quad (1)$$

$$O_2 + 2H^+ + 2e^- \rightarrow H_2O_2 \quad (2)$$

$$Fe^{3+} + e^- \rightarrow Fe^{2+} \quad (3)$$

However, some major challenges are commonly encountered when usingconventional EF process. For instance EF is only optimal at very narrow pH range (pH 2.5 – 3.5), as such working outside this pH drastically reduces the efficiency of the process[11–14]. This is not beneficial when treating real industrial effluents/wastewater, which usually have divergent pH depending on the origin. Further, the catalyst in conventional EF has limited recyclability and reusability and effluent must be neutralized before disposal to nullify the acidic condition, which may also results in generation of sludge that may require a secondary process for its disposal [11,13].

Heterogeneous EF (HEF) process has been developed to overcome these challenges since it is effective over a wide pH range, including basic pH, with recyclability of the solid catalyst [13]. Also, the need for post-treatment neutralization and formation of iron-rich sludge encounter in conventional EF system is completely eliminated with the use of solid catalyst. Based on literature, heterogeneous catalysts such as natural Fe minerals [15–19], supported transition metal/metal oxides [11,20–24], and transition metals doped – carbon aerogel [25–28] have been studied for degradation of the various class of organic pollutants. Excellent mineralization of organics as a result of both homogeneous and surface catalyzed process has been reported for iron containing minerals as heterogeneous catalysts in HEF especially at acid pH, however such system demonstrated low recyclability. Fe/Fe-oxides supported on micro/mesoporous materials have been reported to show high adsorption property for some pollutants which hinders and delays their catalytic degradation by HEF process [29]. Although studies have shown that carbon aerogel doped withtransition metals/oxides exhibited high catalytic activity and reusability over wide pH range; theirintricate and multi-steps preparation route seemsuneconomical for large scale production [25,26]. Recently we reported excellent performance of CoFe-layered double hydroxide (LDH) modified carbon-felt cathode for mineralization of acid-orange II [14], but the

use of Cu and Co as catalyst in HEF is detrimental because both are considered toxic. In fact, leaching of Co or Cu at acidic and neutral pH has been reported for doped carbon aerogel and LDH applied in HEF process [14,25,26,30].

SMT is one of the most widely used sulfonamide antibiotics against aerobic bacteria and protozoa and its combination with other antibiotics is largely administered for the treatment of respiratory disease like pneumonia [31,32]. Several studies have reported the occurrence of SMT at different concentration levels (ng L^{-1} to μg L^{-1}) in various municipal sewage treatment plants (STPs), surface water and even drinking water, however higher concentration levels could be found in untreated hospital effluents, animal impoundments and wastewater effluents from pharmaceutical plants [33,34]. Similarto other pharmaceuticals, the presence of SMT has become a serious environmental concern due to its continuous accumulation and resistance to natural attenuation processes [35]. SMT is refractory to the conventional treatment used in STPs, but many advanced oxidation processes (AOPs) have been applied as an alternative treatment for the degradation of SMT[32]. Among the AOPs, EAOPs such as electrooxidation (EO) and EF have been reported to achieve excellent decontamination of SMT solution [31,32,35].

In this study, $Fe^{II}Fe^{III}$ was deposited on CF by solvothermal process. The prepared cathode was characterized by X-ray diffraction (XRD) measurement, Scanning electron microscopy (SEM), Fourier-transform infrared spectroscopy (FTIR), X-ray photoelectron spectroscopy (XPS) and Electrochemical impedance spectroscopy (EIS) to examineitstructural and electrochemical properties. The catalytic activity of the $Fe^{II}Fe^{III}$ LDH modified CF cathode for total decontamination of synthetic organic polluted wastewater was evaluated by studying the HEF mineralization of SMT (as model pollutants) at pH 3 – 9. Besides, sub-stoichiometric titanium oxide (Ti_4O_7) was used as the anode material. This electrode has been demonstrated to

be efficient in electrochemical wastewater treatment and capable of producing heterogeneous hydroxyl radical ($Ti_4O_7(^{\bullet}OH)$)at it surface via water oxidation (eq. 4) for mineralization of organics, which can contribute to the overall efficiency of the HEF process[36–38].

$$Ti_4O_7 + H_2O \rightarrow Ti_4O_7(^{\bullet}OH) + H^+ + e^- \quad (4)$$

In addition, the evolution of the toxicity of the SMT solution during the HEF treatment was examined using Microtox® method.

2. Materials and methods

2.1 Chemicals

CF was supplied by Alfa Aesar. Iron II sulfate heptahydrate, $FeSO_4.7H_2O$ (> 99% purity); iron III nitrate nonahydrate, $Fe(NO_3)_3.9H_2O$ (98% purity); urea, $CO(NH_2)_2$ and ammonium fluoride, NH_4F (99% purity) were purchased from Sigma Aldrich and utilizedas-supplied for the preparation of LDH deposited on the CF. SMT, $C_{10}H_{11}N_3O_3S$ and sodium sulfate, Na_2SO_4 (anhydrous, 99-100%) were also supplied by Sigma Aldrich. Bioluminescent bacteria *Vibrio fischeri* and the activation reagent LCK 487 LUMISTOX used in Microtox® were supplied by Hach Lange France SAS. All solutions were prepared with ultra-pure water obtained from a Millipore Mill-Q system (R> 18 MΩ cm). Organic solvents and other chemicals used were either HPLC or analytic grade from Sigma-Aldrich, Fluka and Merck.

2.2 Electrode preparation

The $Fe^{II}Fe^{III}$ LDH/CF cathode was produced by *in-situ* solvothermal process using Teflon lining autoclave [14,39–41]. Growth solution was made by dissolving $FeSO_4.7H_2O$ (25 mM), $Fe_2(NO_3)_3.9H_2O$ (12.5 mM), NH_4F (125 mM) and $CO(NH_2)_2$ (0.5 M) in 75 mL of ultra-pure water. A 6 cm × 1 cm × 1.27 cm CF was pretreated with concentrated HNO_3, clean thoroughly using ultrasonication, in a bath containing deionized water, acetone, ethanol and deionized water in the sequence order. Subsequently, the pretreated CF and the homogeneous growth solution was transferred into a Teflon-lined stainless steel autoclave for hydrothermal treatment at ~ 100 ^{0}C. The CF coated with LDH and the LDH particles were carefully removed from the solution, thoroughly washed with water and dried at 60 ^{0}C. The mass-loading of $Fe^{II}Fe^{III}$ LDH coating was accurately measured from the weight difference of dried clean substrate before and after the growth; and the average loading was 0.6 ± 0.02 mg cm^{-2}.

2.3 Electrode characterization

The SEM micrographs of as-prepared cathode weretaken using Hitachi S-4800 microscope. The XRD patterns were collectedusing a BRUKER S5000 diffractometer, using Cu-Kα radiation (0.15418 nm) at 40 kV and 20 mA. FTIR Spectra of the powder LDH was performed on NEXUS FTIR (ThermoFisher). The XPS spectra of the LDH were collected on aESCALAB 250 Thermal Electron using Al*Kα* (1486.6 eV). EIS experiments were conducted in 50 mM Na_2SO_4 solution using μ3AUT70466 Autolab System with a three-electrode cell. The working electrode was the modified CF, whereas Pt foil and Standard Calomel Electrode were used as a counter and reference electrode respectively. Electrical conductivity of the prepared $Fe^{II}Fe^{III}$ LDH/CF was determined by measuring the electrode interfacial charge-transfer

resistance (R_t) using EIS spectra. The impedance spectra were recorded at the open circuit voltage inthe range of 50 kHz to 100 MHz and voltage amplitude of 10 mV.

2.4 EF experiment

The EF trials were conducted in an undivided cylindrical reactor of diameter 4 cm and 150 mL volume equipped with 24 cm^2thin film Ti_4O_7 anode (Saint Gobain C.R.E.E., France), placed in parallel to the cathode (4.5 cm × 1 cm × 1.27 cm) made of $Fe^{II}Fe^{III}$ LDH/CF at approximately 2 cm inter-electrode distance. Single chamber electrochemical cells are easy to operate and the parameters can be easily scale-up to pre-pilot or pilot scale. All electrolyses were carried out with 145 mL SMT solutions (0.2 mM) containing 0.05 M Na_2SO_4 as background electrolyte with constant stirringusing a PTFE magnetic bar. Compressed air was continuously sparged into the reactor at about 1 L min^{-1}, starting at 10 min before electrolysis to ensure a stationary O_2 concentration level. The use of compressed air is normally prefer to pure O_2 especially when using cathode materials with high potential for O_2 reduction reaction such as carbon-felt because of economic advantage and possible scale-up of the process. For comparison, analogous experiments were performed with raw carbon-felt cathode of similar size with the addition of 0.2 mM Fe^{2+} (EF-Fe^{2+}) or without addition of any catalyst (EO-H_2O_2). All electrochemical experiments were performed in duplicate and average values were reported with corresponding error bar.

2.5 Instruments and analytic procedures

All experiments were conducted with a Hameg HM7042-5 triple power supply at constant current density of 7.5 mA cm^{-2}. The SMT solution pH was adjusted with 1 M H_2SO_4 or NaOH and was recorded on a CyberScan pH 1500 pH-meter from Eutech Instruments. The mineralization of the SMT solutions was assessed from the decay of its total organic carbon (TOC). The TOC of samples were analyzed on a Shimadzu TOC-L CSH/CSN analyzer. Reproducible TOC values with ± 2% accuracy were found by injecting 50 μL aliquots into the analyzer. Percentage of TOC removal was calculated from to the following equation:

$$\text{TOC removal (\%)} = \frac{\Delta(\text{TOC})_{\text{exp}}}{\text{TOC}_0} \text{ x } 100 \qquad \text{(eq. 5)}$$

where $\Delta(\text{TOC})_{\text{exp}}$ is the TOC decay at time t (mg L^{-1}) and TOC_o is the corresponding initial value before electrolysis (in same unity).

The decay of SMT concentration was followed by injecting 20 μL aliquots to the reversed-phase high performance liquid chromatography (HPLC) (Dionex) equipped with P680 HPLC pump and fitted with a Purosher RP-18, 5μm, 25 cm × 4.6 mm (i.d.) column at 40 ^oC. Detection was done with a UVD340U photodiode array detector selected at λ = 270 nm. Isocratic solvent mixture of methanol/water (containing 1% H_3PO_4) 25:75 (v/v) was used as mobile phase at a flow rate of 0.8 mL min^{-1}.The quantity of Fe^{2+} and total Fe leached into the treated solution from the $Fe^{II}Fe^{III}$ LDH/CF cathode at pH 3, 6 and 9 was estimated by colorimetric technique in accordance with recipe reported elsewhere [42].

Short-chain carboxylic acids formed during the HEF treatment at pH 3 with $Fe^{II}Fe^{III}$ LDH/CF cathode were analyzed by ion-exclusion HPLC (Merck Lachrom) equipped with a L-2130 pump, a C18 Acclaim OA, 4 mm × 25 cm (i.d.) column at 40 ^oC, and a L-2400 UV detector operated at λ= 210 nm, using 1% H_2SO_4 at 0.2 mL min^{-1} as mobile phase. Aromatic

intermediates produced after 30 min of HEF treatment of 0.5 mM SMT solutions at pH 3 were identified by GC-MS using Trace 1300 gas chromatograph-Single Quadrupole ISQ mass spectrophotometer according to method reported elsewhere [43]. The changein toxicity of the treated SMT solution was studied by measuring the inhibition of the bio-luminescence of the bacteria *Allivibrio fischeri* formerly known as *Vibrio fischeri* using Microtox® method. The pH of all the samples and blank was adjusted to 6.5 – 7.5 with the aid of 0.01 – 0.1 mM NaOH solution prior to Microtox analysis as described elsewhere [44].

3. Results and discussions

3.1 Electrode preparation

The $Fe^{II}Fe^{III}$ LDH modified CF electrode was made by *on*-site solvothermal synthesis [14,40] using urea and ammonium fluoride as precipitation agent. Multiwall of $Fe^{II}Fe^{III}$ LDH was deposited on CF during hydrothermal treatment at 100 ^{o}C. During the hydrothermal treatment, there is gradual decomposition of $CO(NH_2)_2$ (eq. 6) and hydrolysis of NH_4F (eq. 7) which gradually increases the pH of the solution towards basic pH, thus inducing simultaneous nucleation, crystallization and growth of the metallic hydroxides on the CF substrate [14]. The reactions at the hydrothermal temperature are given in eq. 6 – 8:

$$CO(NH_2)_{2(aq)} + 3H_2O_{(l)} + \Delta heat \rightarrow 2NH_4^+{}_{(aq)} + 2OH^-{}_{(aq)} + CO_{2(g)} \quad (6)$$

$$NH_4F_{(aq)} + H_2O_{(l)} \rightarrow NH_4^+{}_{(aq)} + OH^-{}_{(aq)} + HF_{(aq)} \quad (7)$$

$$Fe^{2+}{}_{(aq)} + Fe^{3+}{}_{(aq)} + OH^-{}_{(aq)} \rightarrow Fe^{II}Fe^{III}\ LDH_{(s)} \quad (8)$$

The nucleation and growth of the LDH occurs majorly at the surface and within the CF immersed in the growth solution and the wall of the Teflon because both are high energy regions compared to the bulk of the solution [14].

3.2 electrode characterization

The morphology of the raw and prepared modified cathode analyzed by SEM is shown in Fig. 1. The pretreated raw CF was cleaned and free from dirt as shown in Fig. 1a and 1b. Bysimple hydrothermal approach in Fe^{2+} and Fe^{3+} growth solution, extensive growth of dense platelets of $Fe^{II}Fe^{III}$ LDH covered each strands of the CF (Fig. 1c). A magnified image of Fig. 1c shows a rough, uneven and porous structure with more secondary phase precipitated along with the $Fe^{II}Fe^{III}$ LDH (Fig. 1d) [45].

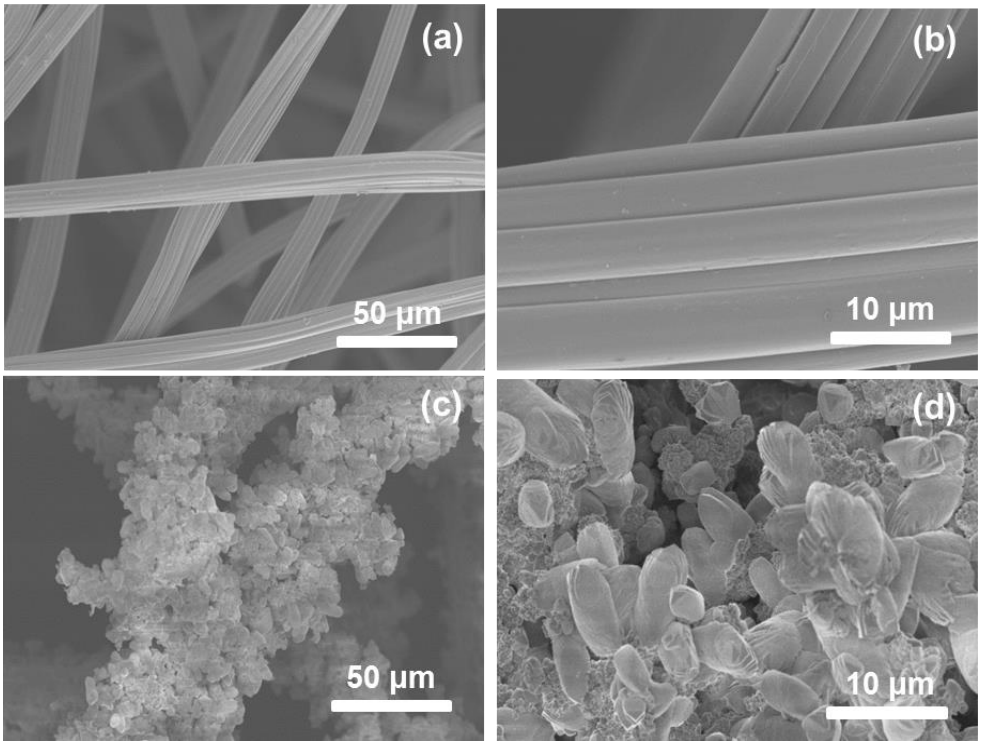

Figure 1: SEM images of (a,b) pretreated raw CF, and (c,d) $Fe^{II}Fe^{III}$ LDH/CF

Crystallinity of the prepared LDH modified CF as well as LDH powder were examined by XRD and showed in Fig. 2a. The XRD patterns of the powders and the modified CF indicated characteristics peaks corresponding to crystal planes of a typical hydrotalcite-like phase [46]. The diffraction peaks (2θ = 6º, 12º, 18º, 23º and 33º) in Fig. 2a represent a typical layered structure with the peaks corresponding to *00l*plane of hydrotalcite-like phase, along with extensive growth of the crystal as depicted by the peaks between2θ of 30º and 55º. The$Fe^{II}Fe^{III}$ LDH crystal showed a good symmetry as depicted by couple of peaks at 57º and 59º 2θ (Fig. 2a). Additionally, the presence of some secondary phases in $Fe^{II}Fe^{III}$LDH was shown by the diffraction peaks at 22º, 31º, 36º and 62º 2θ, corresponding to $Fe(OH)_3$, Fe_2O_3, maghemite Fe_2O_3 and transformation between $Fe(OH)_3$ and Fe_2O_3 respectively [46,47], which is in agreement with the SEM images (Fig. 1d). The peaks around 23º and 43º in lower diffractogram of Fig. 2aare ascribed to the carbon of the CF. Besides, low intensity peaks was observed with LDH modified CF compared to that of LDH powder.

The FTIR spectrum of the $Fe^{II}Fe^{III}$ LDH powder (Fig. 2b) shows two absorption bands at 3750 cm^{-1} and 3700 cm^{-1} assigned to stretching vibration of non-hydrogen and hydrogen bond hydroxyl groups in the octahedral sheet and interlayer of the $Fe^{II}Fe^{III}$ LDH. The peak observed at 1650 cm^{-1} was ascribedto the bending vibration of absorbed water molecule onto the $Fe^{II}Fe^{III}$ LDH. An intense peak at 1379 cm^{-1} was due to the N–O stretching mode of the surface adsorbed nitrate counter anions, which were incorporated primarily from $Fe(NO_3)_3.9H_2O$ of the starting solution [45]. Besides, the bands between 580 – 800 cm^{-1}wavelength could be ascribed to stretching vibration of M–OH and M–O bonds (M = Fe) in the LDH [48].

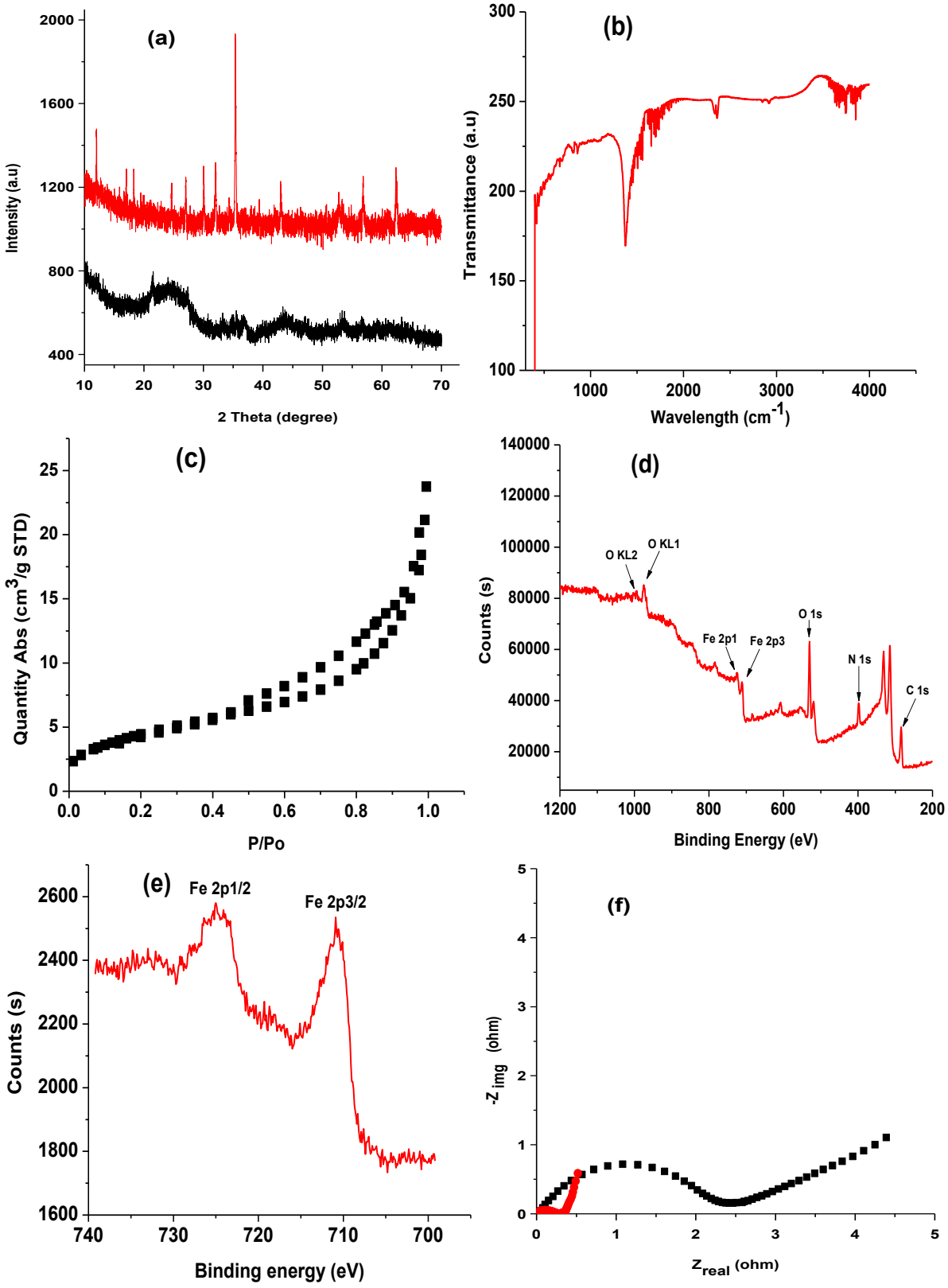
(a)
Intensity (a.u)
2 Theta (degree)
(b)
Transmittance (a.u)
Wavelength (cm-1)
(c)
Quantity Abs (cm3/g STD)
P/Po
(d)
Counts (s)
O KL2
O KL1
Fe 2p1
Fe 2p3
O 1s
N 1s
C 1s
Binding Energy (eV)
(e)
Fe 2p1/2
Fe 2p3/2
Counts (s)
Binding energy (eV)
(f)
-Z img (ohm)
Z real (ohm)

Figure 2: X-ray diffraction patterns of (a) $Fe^{II}Fe^{III}$ LDH powder (upper diffractogram) and $Fe^{II}Fe^{III}$ LDH/CF (lower diffractogram), (b) FTIR spectrum of $Fe^{II}Fe^{III}$ LDH powder, (c) N_2 adsorption isotherm of $Fe^{II}Fe^{III}$ LDH powder and, (d) XPS core level spectra of $Fe^{II}Fe^{III}$ LDH/CF, (e)XPS spectra of Fe 2p of $Fe^{II}Fe^{III}$ LDH/CF and (f) EIS spectra of (■) raw CF and (●)$Fe^{II}Fe^{III}$ LDH/CF obtained at 10 mV and 50 kHz – 100 MHz.

The N_2 adsorption isotherm of the $Fe^{II}Fe^{III}$LDH powder is shown in Fig. 2c, exhibiting type IV isotherm with regular pores as demonstrated by the adsorption-desorption plot. Additionally, the BET surface area of the $Fe^{II}Fe^{III}$ LDH powder was 16.5 m^2 g^{-1}. The XPS spectra of the $Fe^{II}Fe^{III}$ LDH/CF is shown in Fig. 2d and 2e. The XPS core level spectra (2d)) showed the existential state of elements like oxygen (KL and 1s), Fe (2p1/2 and 2p3/2), N (1s) as well as C (1s) indicating successful modification of CF. More so, the Fe 2p core lines split into 2p½ (725 eV) and 2p3/2 (711 eV) peaks (Fig. 2e) with the both peaks accompanied by a small satellite band at around 732 eV and 720 respectively [14].The electrical conductivity and potential of electron transfer capacity of the synthesized $Fe^{II}Fe^{III}$ LDH modified CF as well as raw CF was examined by EIS and presented in Fig. 2f. The interfacial charge-transfer resistance (Rc_t) was presented as suppressed semicircle arcs by the Nyquist plots with the diameter of the semicircle represent the actual value of the Rc_t. It is obvious from Fig. 2f that there was tremendous decrease in the interfacial resistance after the deposition of the $Fe^{II}Fe^{III}$ LDH, indicating significant enhancement in electron transfer and electrical conductivity of the electrode. This could enhance the activity of the prepared cathode in terms of H_2O_2 production as well as Fe^{II}/Fe^{III} or Fe^{3+}/Fe^{2+} redox regeneration [49].

3.3 Mineralization and degradation of SMT: Effect of pH and cathode

The catalytic activity of the as-prepared $Fe^{II}Fe^{III}$ modified CF cathode for the efficient electrochemical wastewater treatment over a wide pH range (pH 3 – 9) was investigated by studying the degradation and mineralization of the antibiotic SMT as a model pollutant. It is worthy to state that the LDH/CF as well as the pretreated raw CF showed limited or no adsorption of the SMT with less than 1% TOC abatement after 8 h in control experiment. HEF treatment with $Fe^{II}Fe^{III}$ LDH/CF cathode showed almost complete mineralization of SMT solutions over the pH range studied at applied current density of 7.5 mA cm^{-2} (Fig. 3a). In fact the initial pH of the treated solution has limited influence on the mineralization of SMT solutions during the HEF treatment. For instance, mineralization efficiency of 97%, 93% and 90% was achieved during HEF treatment with $Fe^{II}Fe^{III}$ LDH/CF at pH 3, 6 and 9 respectively after 8 h of electrolysis, demonstrating the higher efficiency of this process compared to either EO-H_2O_2 and EF-Fe^{2+} at all pH studied (Fig. 4). The excellent mineralization of SMT achieved with $Fe^{II}Fe^{III}$ LDH/CF at both acidic and basic pH can be attributed to surface catalyzed decomposition of H_2O_2 to produced $^{\bullet}OH$ which can easily oxidized SMT and its oxidation intermediates[13,18]. The surface catalyzed process widening the pH window at which HEF can be carried out without necessarily reduced the efficiency of the process because the reaction occurs at solid-liquid interface in the treated solution. As shown in Figs. 3a and 4, less than 10% reduction in TOC removal efficiency was observed when the pH of the treated solution was increased from pH 3 to pH 9. Besides, the surface catalyzed process eliminates the formation of iron hydroxide sludge encountered in homogeneous EF since there was limited leaching of Fe from LDH at basic pH and the solution treated with LDH modified CF remained clear regardless of the initial solution

pH. It is important to state that at acidic pH (*i.e.* pH 3), the oxidation of SMT was by both surface catalyzed process at the surface of the modified cathode and EF-Fe^{2+} oxidation arisen from the leaching of Fe^{3+}/Fe^{2+} from the LDH into the treated solution, in addition to $Ti_4O_7(^{\bullet}OH)$ generated at the anode surface via water oxidation reaction (eq. 4). The leached Fe^{3+}/Fe^{2+} can catalyzed the decomposition of H_2O_2 to produce $^{\bullet}OH$ in Fenton's reaction (eq. 1). The leaching of Fe ions species from the LDH and the quantity leached was confirmed and estimated by colorimetric method and detailed in section 3.3.

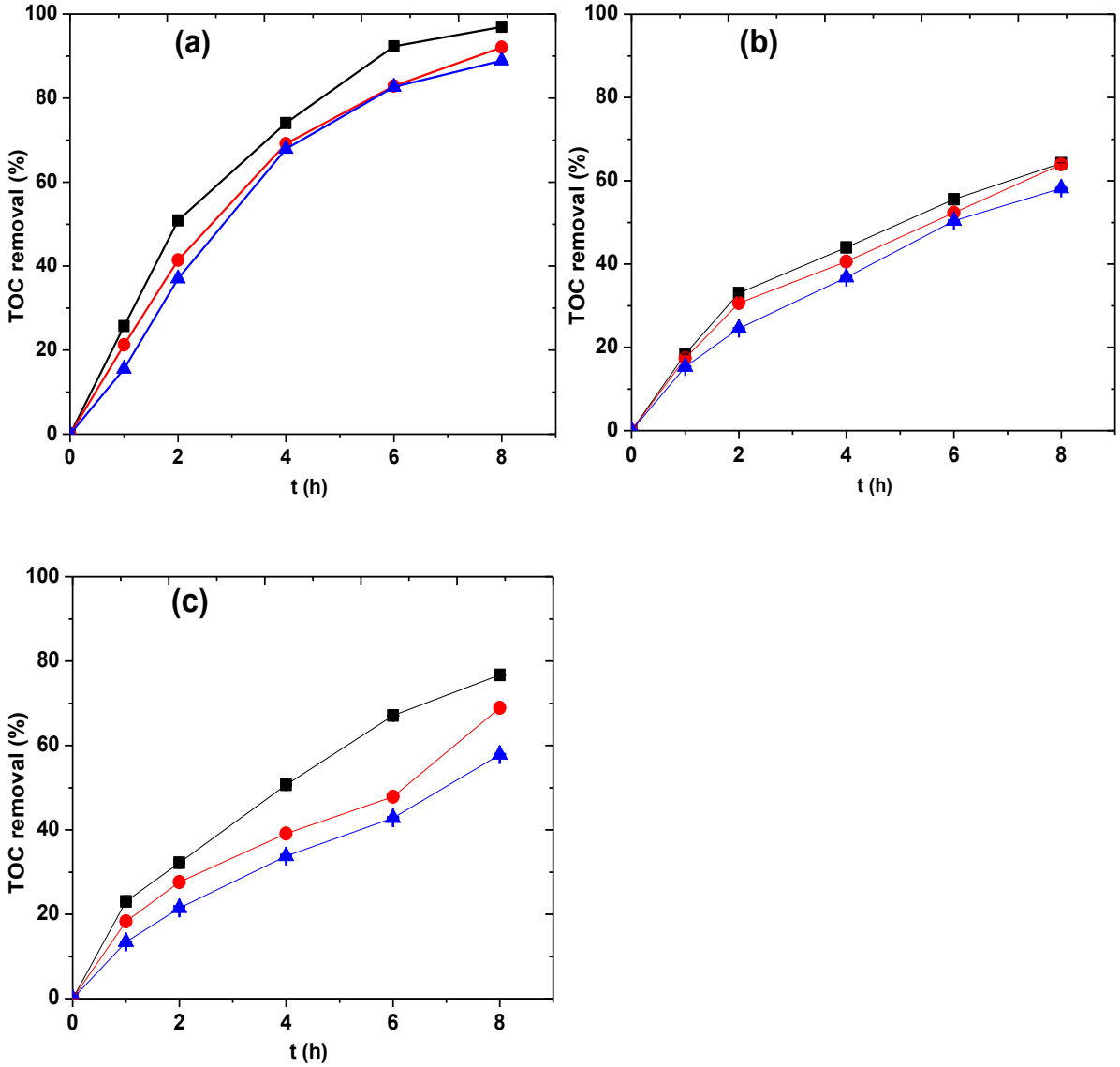

Figure 3: TOC removal efficiency *vs* time during the mineralization of 24 mg L^{-1} TOC SMT solution at: (■) pH 3, (●) pH 6 and (▲) pH 9 and current density of 7.5 mA cm^{-2} using (a) HEF with $Fe^{II}Fe^{III}$ LDH/CF cathode, (b) EO-$H_2O_2$and (c)EF-Fe^{2+} (RSD: < 2%). Anode: Ti_4O_7

Comparatively, the mineralization of SMT studied with zero catalyst addition (*i.e.* EO-H_2O_2) using pretreated raw CF as cathode and Ti_4O_7 anode showedmoderate TOC removal efficiency (Fig. 3b) at all pH studied, achieving 64%, 63% and 53% TOC removal at pH 3, 6 and 9 respectively after 8 h of electrolysis. This clearly shows that the modification of the cathode contributed more than 30% of the mineralization achieved in HEF process. The mineralization of SMT in this case was mainly by physisorbed Ti_4O_7($^{\bullet}$OH) generated at the surface of the Ti_4O_7 anode since no catalyst was added to the treated solutions, as such no $^{\bullet}$OH production in the bulk solution [43,50,51]. Upon addition of optimized catalytic quantity of iron (0.2 mM Fe^{2+}) [30,50] to the treated solutions (*i.e.* EF-Fe^{2+}), an enhanced mineralization of SMT solution was achieved with TOC removal efficiency of 77%, 69% and 58% achieved at pH 3, 6 and 9 respectively (Fig. 3c). This enhanced mineralization of SMT was expected because of the contribution of homogeneously generated $^{\bullet}$OH from Fenton's reaction (eq. 1) between electrogenerated H_2O_2 produced at the cathode and catalytic Fe^{2+} added to the solution prior to treatment [52,53].The TOC removal efficiency during classical EF treatment was significantly reduced with increase in pH majorly due to the precipitation of the Fe^{2+} as hydroxides. In fact, the treated solutions at pH 6 and 9 remained yellow throughout electrolysis time, indicating the continuous presence of iron hydroxides in the solution; and the mineralization attained at these pHs was majorly by Ti_4O_7($^{\bullet}$OH) generated at the surface of the anode. In all cases, the mineralization efficiency obtained with $Fe^{II}Fe^{III}$ LDH/CF was always higher at all electrolysis time and pH values

compared to EO-H_2O_2 or EF-Fe^{2+} as depicted in Fig. 4. More so, the HEF with $Fe^{II}Fe^{III}$ LDH/CF could be an interesting technique for treatment of industrial effluents, especially those from textile and petrochemical industries with higher organic loading (> 3000 mg COD L^{-1}) and varying pH [5] since the efficiency of the process was marginally affect by pH.

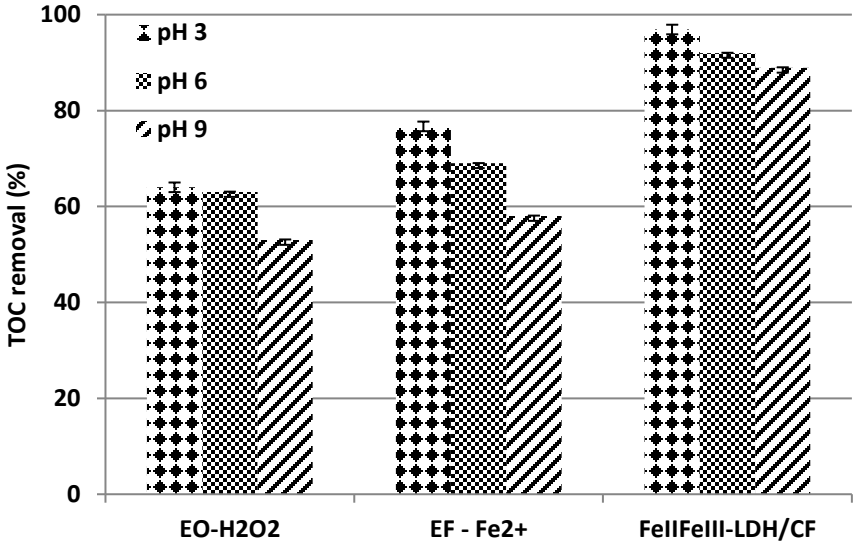

Figure 4: Comparison of the mineralization efficiency at different pHs for the treatment of 24 mg L^{-1} TOC SMT solution at current density of 7.5 mA cm^{-2} using EO-H_2O_2, EF-Fe^{2+}, HEF and $Fe^{II}Fe^{III}$ LDH/CF after 8 h of electrolysis. Anode Ti_4O_7

Fig. 5 showed the corresponding SMT concentration decay with electrolysis time for all the trials of Fig. 3. Complete degradation of SMT was attained in all trials with time required for completeoxidation of SMT increases with pH for all the processes studied. As can be seen in Fig. 5,excellent degradation efficiency was obtained during HEF process with $Fe^{II}Fe^{III}$/CF compared to EO-H_2O_2 and EF-Fe^{2+} at analogous experimental conditions. For example, complete degradation of 0.2 mM SMT solution was achieved after 40, 120 and 240 min at pH 3, 6 and 9

respectively, during HEF with $Fe^{II}Fe^{III}$/CF, whereas it requires over 120, 240 and 360 min; and 60, 240 and 360 min to obtained complete destruction of SMT with EO-H_2O_2 and EF-Fe^{2+} at pH 3, 6 and 9 respectively. The much slower degradation rate observed during EO-H_2O_2 (without Fe^{2+}) (Fig.5b) compared to EF–Fe^{2+} or HEFcan be explained by the fact that the Ti_4O_7(•OH) are produced and confined to the anode region only, thus oxidation of SMT was mainly diffusion controlled [54]. Besides, at higher pH (pH 6 and 9) slower degradation was observed with EF-Fe^{2+} (Fig. 5c), which could be explained by the precipitation of the Fe^{2+} (catalyst) as ferric hydroxide from the solution, reducing the catalytic generation of •OH via Fenton's reaction. Indeed, both the degradation and mineralization of SMT solution at these pHs were predominantly by Ti_4O_7(•OH) generated at the anode via water oxidation.

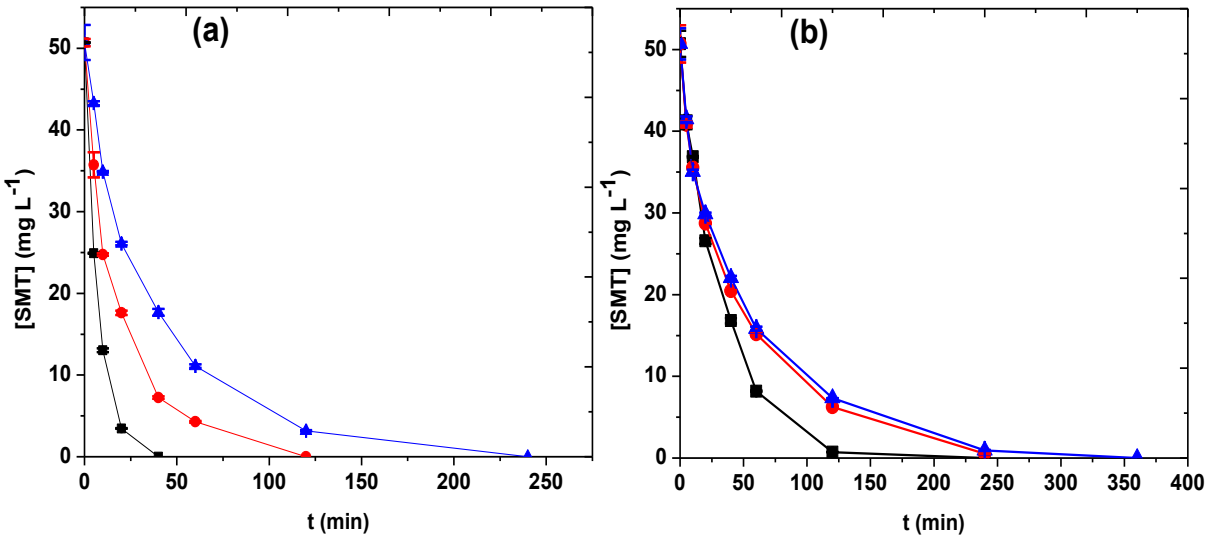

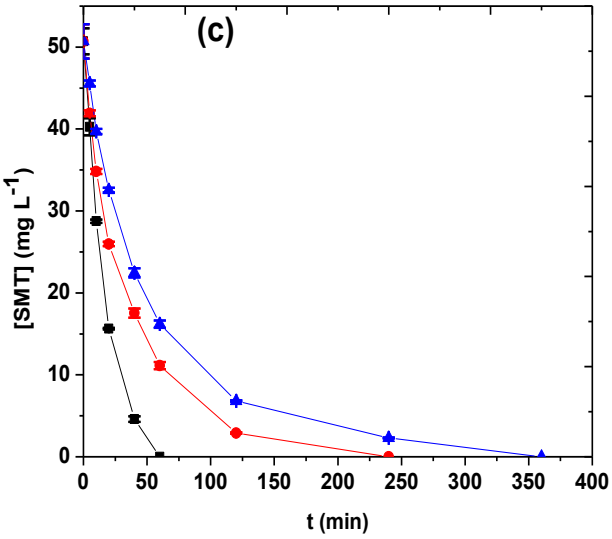

Figure 5: Concentration decay *vs* electrolysis time during the degradation of 50.7 mg L^{-1} (0.2 mM) SMT at: (■) pH 3 (●) pH 6 and (▲) pH 9 and current density of 7.5 mA cm^{-2} using (a) HEF with $Fe^{II}Fe^{III}$ LDH/CF cathode, (b) EO-$H_2O_2$and (c) EF- Fe^{2+}. Anode: Ti_4O_7

3.4 Evolution of pH and Feleaching during electrolysis

The initial pH of the wastewater and its evolution during electrochemical treatment based on Fenton's chemistry has a significant role on the efficiency of the process because the pH affects the availability of the Fe^{3+}/Fe^{2+}cycles (Fenton catalyst) in the solution. Indeed, Fe^{3+}/Fe^{2+} andother heavy metals precipitate as hydroxides as pH increases towards basic pH values. Additionally, the stability of $Fe^{II}Fe^{III}$ LDH used in HEF depends on the pH of the solution. In general, LDHs are less stable at strong acidic pH but barely affected at high pH values [47]. As such the evolution of pH of the SMT solution during treatment with $Fe^{II}Fe^{III}$ LDH/CF cathode was monitored and reported in Fig. 6a. Firstly, it is important to state that the variation in pH of the bulk from electrode regions due to formation of H^+ and OH^-at the anode and cathode respectively was minimized because of strong stirring during the electrolysis that ensures

homogenization at all time. There was sharp reduction in pH of the treated solution at the early stage of electrolysis when treated SMT solution at initial pH 9, but the solution pH remained almost unchanged after 1 h till the end of the treatment. Similar but gradual reduction in pH of the treated solution was observed at pH 6, but the pH kept nearly constant after 2 h of the treatment. The observed reduction in pH at the early stage of treatment can be attributed formation of short-chain carboxylic acids from the oxidative degradation of SMT and its cyclic byproducts[2,3,6]. In contrast, the pH of the treated solution was stable in case of treated SMT solution at pH 3 (Fig. 6a), except for the early slightly increase observed within the first 10 min of electrolysis which was probably due to the inherited basic condition of preparing the cathode. Note that the change in the pH of the treated SMT solution over the electrolysis time has negligible effect on the cell potential,with variation of less than 0.4 V observed for the three pH values studied (Table 1.)

Table 1: Evolution of cell voltage over electrolysis time during the treatment of SMT solution at different pH values

Time (h)		0	1	2	4	6	8
E_{cell}	pH 3	5.50	5.57	5.55	5.68	5.81	5.80
	pH 6	5.50	5.45	5.43	5.48	5.55	5.63
	pH 9	5.47	5.53	5.43	5.46	5.57	5.64

The quantities of Fe leached from the $Fe^{II}Fe^{III}$ LDH/CF cathode during the treatment of SMT solution at different initial pHs was reported in Fig. 6b. As depicted in Fig 6b, the prepared cathode showed very high stability at high initial SMT solution pH with the total Fe leached from the cathode less than 1 mg L^{-1} and 0.5 mg L^{-1} for the treatment at initial solution pH value of 6 and 9, respectively. This implied that the contribution of homogeneous Fe^{2+}/Fe^{3+} catalyzed

EF to the degradation of SMT solution was negligible and the mineralization of SMT was predominantly by surface catalyzed process at these pH values. However, the LDH became slightly unstable at strong acid pH (*i.e.* pH 3) and significant quantities of Fe (≈ 9 mg L^{-1}) were leached into the treated solution (Fig. 6b), suggesting the participation of EF-Fe^{2+} in the overall mineralization of the SMT solution at pH 3. The leached Fe existed in the solution as Fe^{3+}/Fe^{2+}, which can homogeneously catalyzed H_2O_2 decomposition to produce $^{\bullet}OH$. It is important to note that the Fe^{3+}/Fe^{2+} redox couple were continuously present in the solution, thanks to the formation of Fe^{3+} from Fenton's decomposition of H_2O_2 by Fe^{2+} (eq. 1) and cathodic reduction of Fe^{3+} to Fe^{2+} (eq. 3).

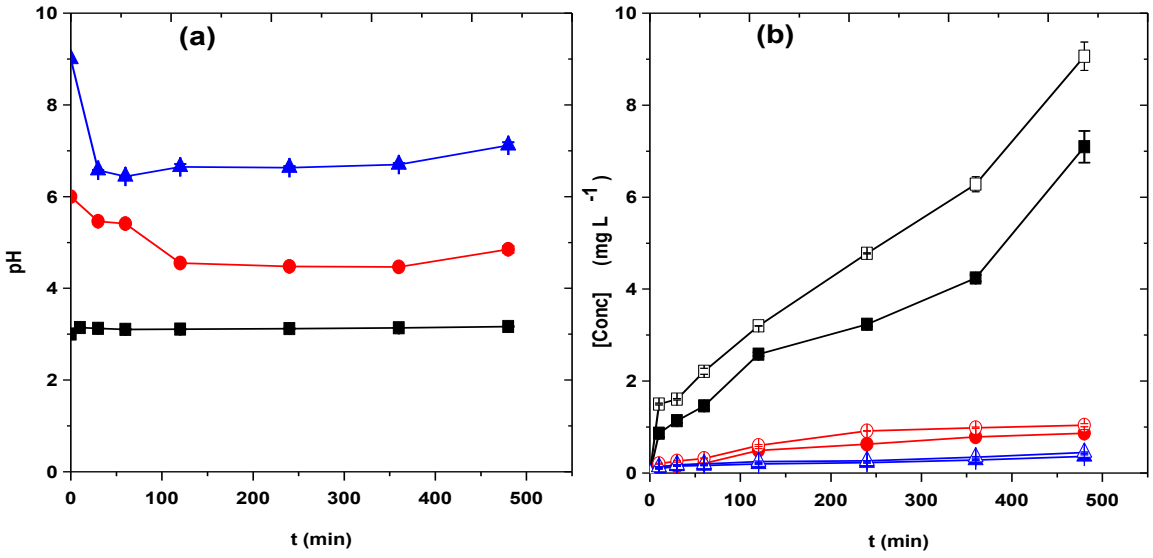

Figure 6: (a) Evolution of pH with electrolysis time: (■) pH 3, (●) pH 6 and (▲) pH 9; and (b) evolution of leached (■,●,▲) Fe^{2+} and (□,○,Δ) Fe_{Total} with electrolysis time at (■,□) pH 3, (●,○) pH 6 and (▲,Δ) pH 9 during the treatment of SMT solution using $Fe^{II}Fe^{III}$ LDH/CF at current density of 7.5 mA cm^{-2}. Anode: Ti_4O_7

3.5 Evolution of oxidation by-products and reaction pathway

The mineralization of organic pollutants by hydroxyl radicals generated in electrochemical oxidation generally involves the formation of several cyclic intermediates and release of inorganic ions with the former further oxidized to C-4 carboxylic acids, which are the final end organic by-products in the treated solution [55]. The carboxylic acid generated during the HEF treatment of 0.2 mM SMT solution at pH 6 and current density of 7.5 mA cm^{-2} using $Fe^{II}Fe^{III}$ LDH/CF cathode was depicted in Fig. 7. Five distinctive peaks were shown on the HPLC chromatograms at 6.8, 8.2, 10.2, 14.3 and 16.4 min identified to be oxalic, maleic, oxamic, glycoxylic and pyruvic acids. This was confirmed by injecting standard solutions of these acids into reversed phase HPLC using an ion-exclusion column. As shown in Fig. 7, accumulation – destruction cycle was observed for all the carboxylic acids, thanks to the rapid formation from oxidation of SMT and its cyclic intermediate at the early stage and mineralization of the acids with the increase in electrolysis time. Oxalic acid was the most accumulated as expected because it is the final end organic byproducts of oxidation of both cyclic and non-cyclic compound [56,57]. Note that, the carboxylic acids found in the final treated solution accounts for the remnant TOC (~7% at pH 6) reported in Fig. 3.

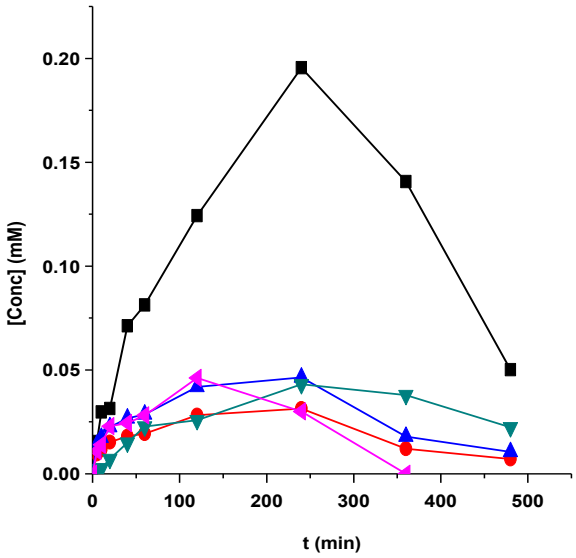

Figure 7: Time course of the main aliphatic carboxylic acids accumulated during HEF treatment of 0.2 mM SMT solution using $Fe^{II}Fe^{III}$ LDH/CF at pH 6 and current density of 7.5 mA cm^{-2}. Acids: (■) oxalic, (●) maleic (▲) oxamic, (▼) glycoxylic and (◀) pyruvic.

The GC-MS analysis of electrolyzed SMT solution after 30 min showed the formation of several aromatic/cyclic intermediates such as hydroxylated SMT (m/z = 267.9), 3-amino-5-methylisoxazole (m/z = 99.09), hydroxylated 3-amino-5-methylisoxazole (m/z = 116.18), 4-amino benzene sulfonamide (m/z = 175), hydroxylated 4-amino benzene sulfonamide (m/z = 191.6), hydroquinone and p-benzoquinone (m/z = 110). The 3-amino-5-methylisoxazole, hydroxylated SMT, hydroxylated 4-amino benzene sulfonamide, hydroquinone and p-benzoquinone have been identified as aromatic intermediate for SMT oxidation by other studies [31,32,58]. Based on these identified cyclic intermediates and the carboxylic acids, a proposed degradation pathway for complete mineralization of SMT by HEF using $Fe^{II}Fe^{III}$ LDH/CF cathode was given in Fig. 8, assuming hydroxyl radicals as the main oxidant. The degradation of

SMT molecules was initiated either by the cleavage of the peptide bond to give 3-amino-5-methylisoxazole and 4-amino benzene sulfonamide or hydroxylation of SMT to hydroxylated SMT which can further undergoes cleavage of the peptide bond like original SMT molecule. Further hydroxylation, deamination and desulfonation of 4-amino benzene sulfonamide give p-benzoquinone which was further oxidized, along with deaminated 3-amino-5-methylisoxazole to several carboxylic acids that were finally mineralized to CO_2 and water.

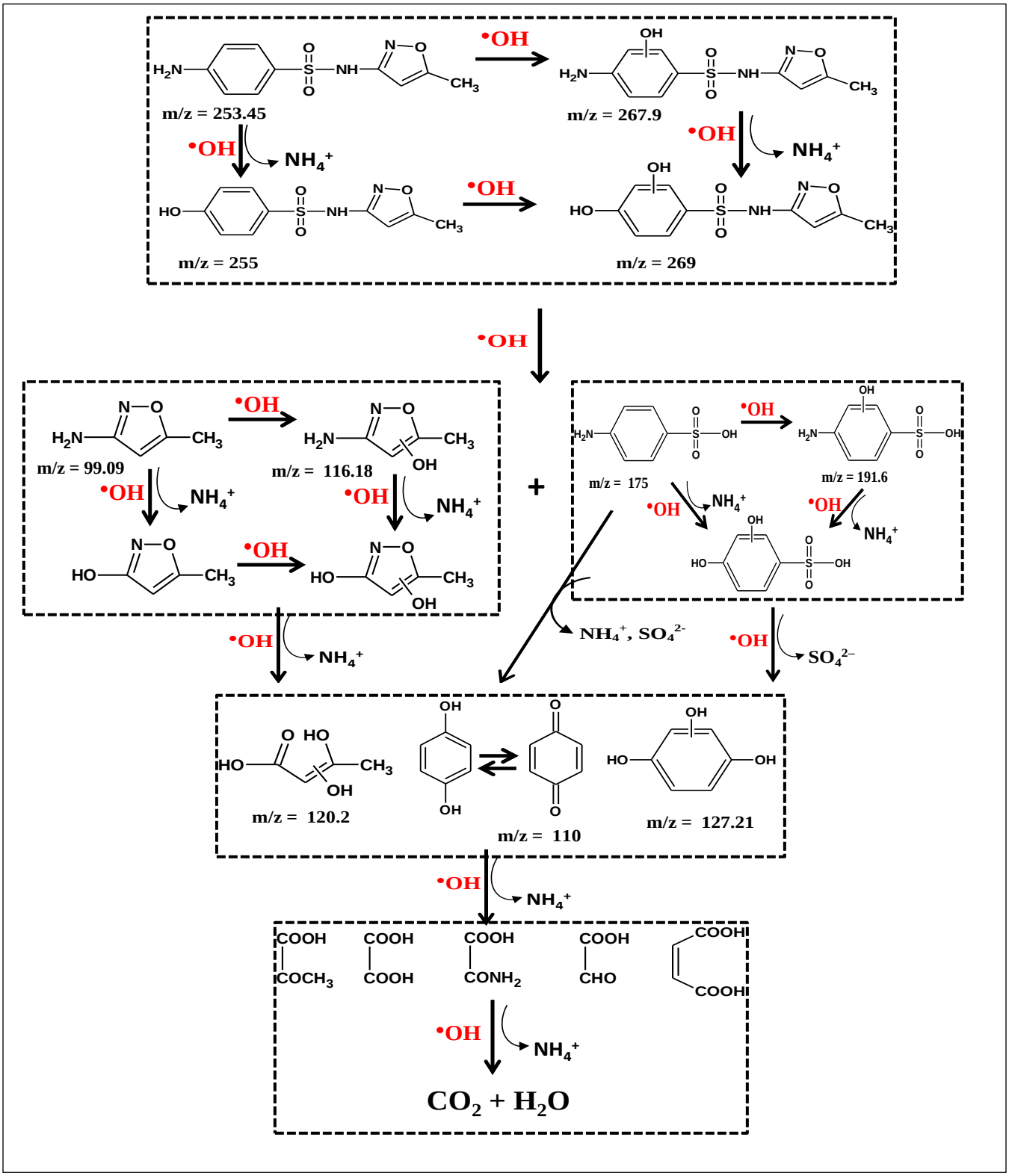
•OH
m/z = 253.45
m/z = 267.9
NH4+
m/z = 255
m/z = 269
m/z = 99.09
m/z = 116.18
m/z = 175
m/z = 191.6
NH4+, SO4 2-
SO4 2–
m/z = 120.2
m/z = 110
m/z = 127.21
COOH
COCH3
CONH2
CHO
CO2 + H2O

Figure 8: Reaction mechanism for complete degradation of SMT molecule assuming •OH as the major oxidant.

3.6Assessment of toxicity and reusability of Fe(II)Fe(III)LDH/CF cathode

The evolution of toxicity of SMT solution with electrolysis time during HEF treatment using $Fe^{II}Fe^{III}$ LDH/CF cathode at pH 3 and 6 was assessed by Microtox® method and reported in Figs. 9a and 9b. The initial SMT solution showed relatively high luminescence inhibition to *V. fischeri* bacteria at the beginning of electrolysis, demonstrating the toxicity of the antibiotic. The % luminescence inhibition quickly increased at the beginning of treatment owing to increased toxicity of the treated solution. Such sharp increase in bacteria inhibition can been attributed to the formation of cyclic byproducts which are more toxic than the parent compounds [53,59]. For treatment at pH 3, the high inhibition lasted up to 40 min of electrolysis before slight reduction and increment to second maximum, indicating the formation of secondary intermediates that are less toxic compared to primary cyclic byproducts. The % inhibition gradually reduced afterward until almost zero inhibition at the end of the treatment (Fig. 9a), demonstrating the total destruction of SMT, primary and secondary cyclic intermediates into biodegradable byproducts (C-4 carboxylic acids) and detoxification of the solution. Similar trend was observed for treatment at pH 6 (Fig. 9b), however the maximum inhibition of *V. fischeri* bacteria luminescenceof treated solution at the early stage of electrolysislasted for longer time (70 min) compared to what was observed at pH 3 (Fig. 9b), indicating slower degradation of aromatic byproducts at pH 6 in comparisonwith pH 3. This agrees well with the TOC removal efficiency reported in Fig. 3a.

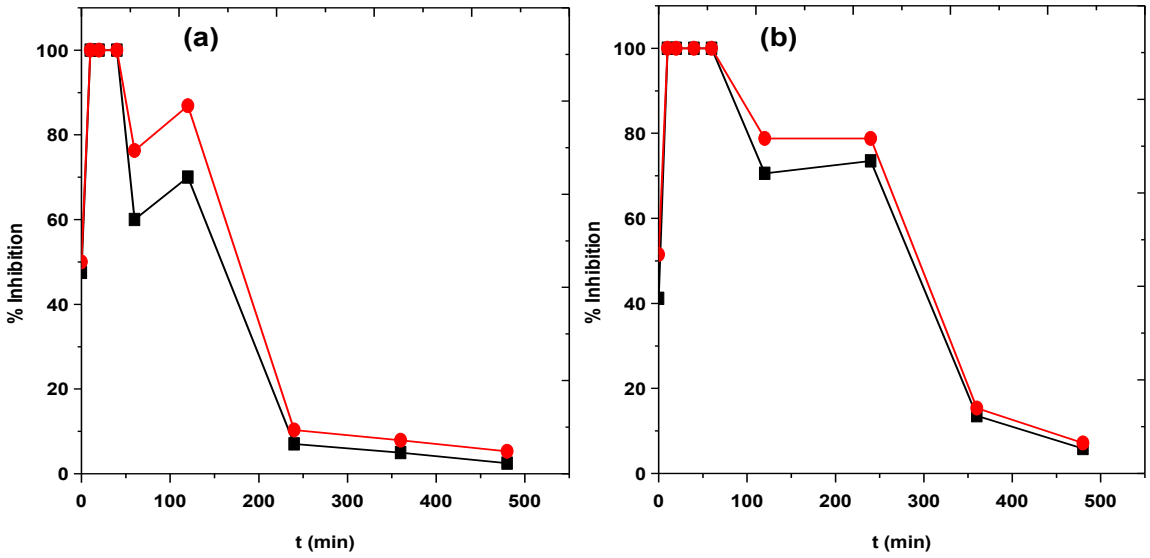

Figure 9: Evolution of % inhibition vs electrolysis time (a) pH 3 and (b) pH 6 after (■) 5 min and (●) 15 min of exposure to *V. fischeri* bacteria

The stability of the catalytic activity and reusability of the prepared $Fe^{II}Fe^{III}$ LDH/CF cathode for the mineralization and degradation of SMT solution at pH 6 was shown in Fig. 10.The stability experiment was performed by replacing the used/treated solution by fresh SMT solution and mildly washing the $Fe^{II}Fe^{III}$ LDH/CF cathode after each cycle.Excellent reusability over 10 cycles of 4 h treatment was observed for both mineralization and degradation of SMT solution. The catalytic efficiency of $Fe^{II}Fe^{III}$ LDH/CF showed less than 17% reduction in term of TOC removal efficiency over 10 cycles of 4 h treatment (Fig. 10a), demonstrating the efficacy of the HEF process for treatment of SMT solution. Interestingly, complete degradation of 0.2 mM SMT was always observed even after 10 cycles as depicted in Fig. 10b, indicating the high stability of the catalytic activity of the prepared cathode. Complete degradation of SMT was attained after 1 h of electrolysis for the first two cycles, whereas it requires over 2 h for the rest

of the cycles, confirming the slight reduction in the catalytic activity of the cathode with reusability. As shown in Fig. 10a, the observed reduction in catalytic activity of the cathode over the 10 cycles was attributed to mechanical wearing of the LDH particles from the carbon-felt due to vigorous stirring, since the LDH is very stable at the working pH (pH 6) as reported in Fig. 6b.

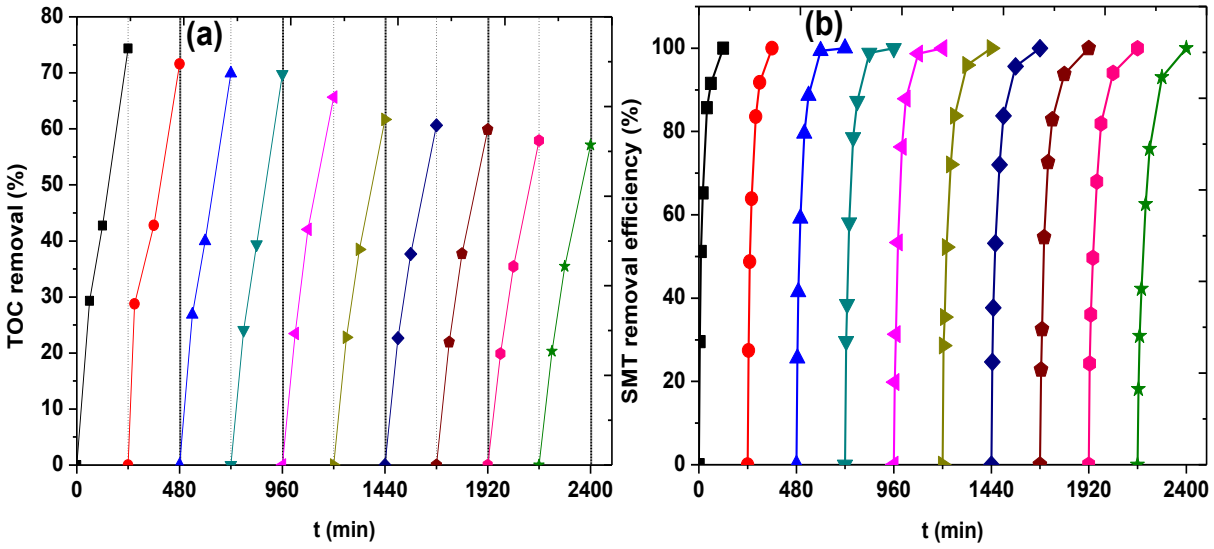

Figure 10: Reusability of $Fe^{II}Fe^{III}$ LDH/CF cathode at pH 6 with cycle (a) TOC removal and (b) SMT removal efficiency during the treatment of 0.2 mM SMT solution using $Fe^{II}Fe^{III}$ LDH/CF at 7.5 mA cm^{-2}.

3.7 Mechanism of mineralization of SMT at different pH

According to the literature [11,13], two different situations may be encounteredduring HEF treatment depending on the pH of the treated solution and solubility of the solid Fe catalyst with pH. At strong acidic pH (*i.e.* pH 3), the production of •OH seems to be controlled by redox cycling of dissolved Fe^{3+}/Fe^{2+} resulting from the leaching of the LDH and surface Fe^{II}/Fe^{III} at the

surface of the LDH. As such the mineralization and degradation of the SMT at pH 3 was a combined contribution of homogeneous and surface catalyzed (heterogeneous) processes, in addition to the oxidation by $Ti_4O_7(^{\bullet}OH)$ generated at the surface of the anode via water oxidation irrespective of pH. The *in-situ* H_2O_2 produced between the cathode and solution interface in acidic medium is catalytically decomposed to stronger oxidizing agent ($^{\bullet}OH$) by the surface bound $\equiv Fe^{II}/Fe^{III}$ or dissolved Fe^{3+}/Fe^{2+} in the bulk.

In contrast, at neutral and basic pH (pH 6 and 9), H_2O_2activation was majorly by surface iron catalyzed process because LDH is almost insoluble at these pHs (Fig. 8b). HEF is a surface-catalyzed process controlled by many parameters such as H_2O_2 concentration, solution pH and solid catalyst properties [13,18]. The kineticsand the reaction mechanism of the heterogeneous catalytic activation of H_2O_2 is not well-resolved in literature; however the formation of $^{\bullet}OH$ from catalytic activation of H_2O_2 by metal oxides is generally accepted as the most critical step in the entire oxidation process, which is similar to that of classical Fenton system as proposed by Harber-Weiss theory [13]. The $^{\bullet}OH$ formation in surface catalyzed process is initiated by interaction of H_2O_2 with the surface iron species like $\equiv Fe^{III}\text{—}OH$ and its one-electron reduced form, $\equiv Fe^{II}\text{—}OH$ (eq. 10), forming a surface complex of H_2O_2, $\equiv Fe^{III}\text{—}OH(H_2O_2)_s$ (eq. 11) at the inner and outer matrix of the carbon-felt[13,18]. The $\equiv Fe^{III}\text{—}OH(H_2O_2)_s$ complex may further undergo a reversible ground-state electron transfer (eq. 12) and activation (eq. 13) to form $\equiv Fe^{II}\text{—}OH$ and $HO_2^{\bullet}$. With the rapid consumption of H^+ in basic medium, the rate of eq. 13 and 14 can be significantly promoted, thus increasing the $^{\bullet}OH$ rate [13]. Beside, this could also explain the excellent mineralization of SMT observed at pH 6 and 9. Accordingly, the $\equiv Fe^{II}\text{—}OH$ catalyzes the activation of H_2O_2 to $^{\bullet}OH$ (eq. 14), which, along with $Ti_4O_7(^{\bullet}OH)$ can mineralize SMT and its intermediates to CO_2 and H_2O (eq. 15). The $^{\bullet}OH$ produced may either react directly

with SMT molecules (eq. 15) or quenched by H_2O_2 (eq. 16) to form weak oxidant $HO_2^{\bullet}$. As such, high mass transport of the organic molecules (stirring) is necessary to ensure maximum reaction of $^{\bullet}OH$ with organic pollutant as well as minimize the scavenging of the $^{\bullet}OH$.

$$\equiv Fe^{III}\text{—}OH + e^{-} \rightarrow \equiv Fe^{II}\text{—}OH \quad (10)$$

$$\equiv Fe^{III}\text{—}OH + H_2O_2 \leftrightarrow \equiv Fe^{III}\text{—}OH(H_2O_2)_{(s)} \quad (11)$$

$$\equiv Fe^{III}\text{—}OH(H_2O_2)_{(s)} \rightarrow \equiv Fe^{II}\text{—}OH(HO_2^{\bullet})_{(s)} + H^{+} \quad (12)$$

$$\equiv Fe^{II}\text{—}OH(HO_2^{\bullet})_{(s)} \rightarrow \equiv Fe^{II}\text{—}OH + HO_2^{\bullet} + H^{+} \quad (13)$$

$$\equiv Fe^{II}\text{—}OH + H_2O_2 \rightarrow \equiv Fe^{III}\text{—}OH + {}^{\bullet}OH + OH^{-} \quad (14)$$

$$^{\bullet}OH/Ti_4O_7(^{\bullet}OH) + SMT \rightarrow CO_2 + H_2O \quad (15)$$

$$^{\bullet}OH + H_2O_2 \rightarrow HO_2^{\bullet} + H_2O \quad (16)$$

4. Conclusions

The oxidative degradation of antibiotic SMT and mineralization of its aqueous solutionin both acidic and basic media by HEF system using $Fe^{II}Fe^{III}$ LDH/CF cathode was investigated. The $Fe^{II}Fe^{III}$ LDH was grown on CF by solvothermal process and the structural, chemical and electrochemical characterization reveals highly crystalline and porous structure containing FeOOH and Fe_2O_3 as major secondary phase with enhanced conductivity. Excellent mineralization of SMT solutions was observed at all pHs studied with TOC removal of at least 90% attained after 8 h of treatment. In contrast, conventional EF with optimized quantity of Fe^{2+} as well as EO-H_2O_2 using raw CF cathode showed lower mineralization of SMT solutions at all

the studied pH values in comparison to HEF with $Fe^{II}Fe^{III}$ LDH/CF cathode. The mineralization of SMT in HEF was by both Fe^{3+}/Fe^{2+} redox homogeneous catalyzed and surface catalyzed processes at strong acidic pH (pH 3), whereas surface catalyzed process was predominant at neutral or basic pH (pH 6 and 9) along with the contribution of $Ti_4O_7(^{\bullet}OH)$ generated at the anode surface irrespective of pH. Catalytic activity of the prepared cathode was highly stable with negligible leaching at high pH and excellent reusability was achieved over 10 cycles of 4 h treatment. The initial SMT solution showed relatively high inhibition to *V. fischeri* bacteria but was totally detoxified to approximately zero percent inhibition after 8 h of treatment using $Fe^{II}Fe^{III}$ LDH/CF at pH 3 as well as pH 6. SMT degradation was *via* the formation of several cyclic intermediates which were later mineralized to short-chain carboxylic acids as the final end organic byproducts in the treated solution. Based on identified intermediate products, a plausible mineralization pathway is proposed. Finally at optimum conditions, effective decontamination of synthetic SMT solution could be achieved within 4 – 6 h electrolysis with minimized energy cost.

ACKNOWLEDGEMENTs

The authors thank the EU for providing financial support through the Erasmus Mundus Joint Doctorate Programme ETeCoS^3 (Environmental Technologies for Contaminated Solids, Soils and Sediments, grant agreement FPA n°2010-0009) and the ANR (French National Research Agency) funding through ANR ECO TS – CELectrON, (grant n°: ANR-13-ECOT-0003).

References

[1] M. Panizza, G. Cerisola, Direct and mediated anodic oxidation of organic pollutants, Chem. Rev. 109 (2009) 6541–6569.

[2] E. Brillas, I. Sires, M.A. Oturan, Electro-Fenton process and related electrochemical technologies based on Fenton's reaction chemistry, Chem. Rev. 109 (2009) 6570–6631.

[3] M.A. Oturan, J.J. Aaron, Advanced oxidation processes in water/wastewater treatment: Principles and applications. A review, Crit. Rev. Environ. Sci. Technol. 44 (2014) 2577–2641.

[4] C.A. Martínez-Huitle, M.A. Rodrigo, I. Sirés, O. Scialdone, Single and coupled electrochemical processes and reactors for the abatement of organic water pollutants: A critical review, Chem. Rev. 115 (2015) 13362–13407.

[5] K.V. Plakas, A.J. Karabelas, Electro-Fenton applications in the water industry, in: Springer Berlin Heidelberg, Berlin, Heidelberg, 2017.

[6] M.A. Rodrigo, N. Oturan, M.A. Oturan, Electrochemically assisted remediation of pesticides in soils and water: A review, Chem. Rev. 114 (2014) 8720–8745.

[7] I. Sirés, E. Brillas, M.A. Oturan, M.A. Rodrigo, M. Panizza, Electrochemical advanced oxidation processes: today and tomorrow. A review, Environ. Sci. Pollut. Res. 21 (2014) 8336–8367.

[8] S.O. Ganiyu, E.D. van Hullebusch, M. Cretin, G. Esposito, M.A. Oturan, Coupling of membrane filtration and advanced oxidation processes for removal of pharmaceutical residues: A critical review, Sep. Purif. Technol. 156 (2015) 891–914.

[9] Z. Niu, Y. Wang, H. Lin, F. Jin, Y. Li, J. Niu, Electrochemically enhanced removal of perfluorinated compounds (PFCs) from aqueous solution by CNTs-graphene composite electrode, Chem. Eng. J. 328 (2017) 228–235.

[10] I. Sirés, E. Brillas, Remediation of water pollution caused by pharmaceutical residues based on electrochemical separation and degradation technologies: A review, Environ. Int. 40 (2012) 212–229.

[11] J. Li, Z. Ai, L. Zhang, Design of a neutral electro-Fenton system with Fe@Fe_2O_3/ACF composite cathode for wastewater treatment, J. Hazard. Mater. 164 (2009) 18–25.

[12] N. Qiao, H. Ma, M. Hu, Design of a neutral three-dimensional electro-Fenton system with various bentonite-based Fe particle electrodes: A comparative study, Mater. Res. Innov. 19 (2015) S2-137-S2-141.

[13] Y. Wang, G. Zhao, S. Chai, H. Zhao, Y. Wang, Three-dimensional homogeneous ferrite-carbon aerogel: One pot fabrication and enhanced electro-Fenton reactivity, ACS Appl. Mater. Interfaces. 5 (2013) 842–852.

[14] S.O. Ganiyu, T.X. Huong Le, M. Bechelany, G. Esposito, E.D. van Hullebusch, M.A. Oturan, M. Cretin, A hierarchical CoFe-layered double hydroxide modified carbon-felt cathode for heterogeneous electro-Fenton process, J Mater Chem A. 5 (2017) 3655–3666.

[15] A. Özcan, A. Atılır Özcan, Y. Demirci, E. Şener, Preparation of Fe_2O_3 modified kaolin and application in heterogeneous electro-catalytic oxidation of enoxacin, Appl. Catal. B Environ. 200 (2017) 361–371.

[16] L. Labiadh, M.A. Oturan, M. Panizza, N.B. Hamadi, S. Ammar, Complete removal of AHPS synthetic dye from water using new electro-fenton oxidation catalyzed by natural pyrite as heterogeneous catalyst, J. Hazard. Mater. 297 (2015) 34–41.

[17] N. Barhoumi, H. Olvera-Vargas, N. Oturan, D. Huguenot, A. Gadri, S. Ammar, E. Brillas, M.A. Oturan, Kinetics of oxidative degradation/mineralization pathways of the antibiotic tetracycline by the novel heterogeneous electro-Fenton process with solid catalyst chalcopyrite, Appl. Catal. B Environ. 209 (2017) 637–647.

[18] G. Zhang, Y. Zhou, F. Yang, FeOOH-catalyzed heterogeneous electro-Fenton system upon anthraquinone@Graphene nanohybrid cathode in a divided electrolytic cell: Catholyte-regulated catalytic oxidation performance and mechanism, J. Electrochem. Soc. 162 (2015) H357–H365.

[19] C.M. Sánchez-Sánchez, E. Expósito, J. Casado, V. Montiel, Goethite as a more effective iron dosage source for mineralization of organic pollutants by electro-Fenton process, Electrochem. Commun. 9 (2007) 19–24.

[20] W.R.P. Barros, J.R. Steter, M.R.V. Lanza, A.C. Tavares, Catalytic activity of Fe3−xCuxO4 ($0 \leq x \leq 0.25$) nanoparticles for the degradation of Amaranth food dye by heterogeneous electro-Fenton process, Appl. Catal. B Environ. 180 (2016) 434–441.

[21] O. Iglesias, M.A.F. de Dios, T. Tavares, M.A. Sanromán, M. Pazos, Heterogeneous electro-Fenton treatment: preparation, characterization and performance in groundwater pesticide removal, J. Ind. Eng. Chem. 27 (2015) 276–282.

[22] C. Zhang, M. Zhou, G. Ren, X. Yu, L. Ma, J. Yang, F. Yu, Heterogeneous electro-Fenton using modified iron–carbon as catalyst for 2,4-dichlorophenol degradation: Influence factors, mechanism and degradation pathway, Water Res. 70 (2015) 414–424.

[23] S.B. Hammouda, F. Fourcade, A. Assadi, I. Soutrel, N. adhoum, A. Amrane, L. Monser, Effective heterogeneous electro-Fenton process for the degradation of a malodorous

compound, indole, using iron loaded alginate beads as a reusable catalyst, Appl. Catal. B Environ. 182 (2016) 47–58.

[24] J. Ramírez, L.A. Godínez, M. Méndez, Y. Meas, F.J. Rodríguez, Heterogeneous photo-electro-Fenton process using different iron supporting materials, J. Appl. Electrochem. 40 (2010) 1729–1736.

[25] H. Zhao, Y. Chen, Q. Peng, Q. Wang, G. Zhao, Catalytic activity of MOF(2Fe/Co)/carbon aerogel for improving H2O2 and OH generation in solar photo–electro–Fenton process, Appl. Catal. B Environ. 203 (2017) 127–137.

[26] H. Zhao, L. Qian, X. Guan, D. Wu, G. Zhao, Continuous bulk FeCuC aerogel with ultradispersed metal nanoparticles: An efficient 3D heterogeneous electro-Fenton cathode over a wide range of pH 3–9, Environ. Sci. Technol. 50 (2016) 5225–5233.

[27] H. Zhao, L. Qian, Y. Chen, Q. Wang, G. Zhao, Selective catalytic two-electron O_2 reduction for onsite efficient oxidation reaction in heterogeneous electro-Fenton process, Chem. Eng. J. 332 (2018) 486–498.

[28] Y. Wang, H. Zhao, G. Zhao, Highly Ordered Mesoporous Fe_3O_4@Carbon Embedded Composite: High Catalytic Activity, Wide pH Range and Stability for Heterogeneous Electro-Fenton, Electroanalysis. 28 (2016) 169–176..

[29] E.G. Garrido-Ramírez, M.L. Mora, J.F. Marco, M.S. Ureta-Zañartu, Characterization of nanostructured allophane clays and their use as support of iron species in a heterogeneous electro-Fenton system, Appl. Clay Sci. 86 (2013) 153–161.

[30] L. Liang, Y. An, M. Zhou, F. Yu, M. Liu, G. Ren, Novel rolling-made gas-diffusion electrode loading trace transition metal for efficient heterogeneous electro-Fenton-like, J. Environ. Chem. Eng. 4 (2016) 4400–4408.

[31] A. Dirany, I. Sirés, N. Oturan, M.A. Oturan, Electrochemical abatement of the antibiotic sulfamethoxazole from water, Chemosphere 81 (2010) 594–602.

[32] Y. Huang, T. Zhou, X. Wu, J. Mao, Efficient sonoelectrochemical decomposition of sulfamethoxazole adopting common Pt/graphite electrodes: The mechanism and favorable pathways, Ultrason. Sonochem. 38 (2017) 735–743.

[33] T.A. Ternes, Occurrence of drugs in German sewage treatment plants and rivers: Dedicated to Professor Dr. Klaus Haberer on the occasion of his 70th birthday.1, Water Res. 32 (1998) 3245–3260.

[34] O. Frédéric, P. Yves, Pharmaceuticals in hospital wastewater: Their ecotoxicity and contribution to the environmental hazardous of the effluent, Chemosphere 115 (2014) 31–39.

[35] H. Lin, J. Niu, J. Xu, Y. Li, Y. Pan, Electrochemical mineralization of sulfamethoxazole by Ti/SnO2-Sb/Ce-PbO2 anode: Kinetics, reaction pathways, and energy cost evolution, Electrochimica Acta. 97 (2013) 167–174.

[36] N. Oturan, S.O. Ganiyu, S. Raffy, M.A. Oturan, Sub-stoichiometric titanium oxide as a new anode material for electro-Fenton process: Application to electrocatalytic destruction of antibiotic amoxicillin, Appl. Catal. B Environ. 217 (2017) 214–223..

[37] A.M. Zaky, B.P. Chaplin, Porous substoichiometric TiO_2 anodes as reactive electrochemical membranes for water treatment, Environ. Sci. Technol. 47 (2013) 6554–6563.

[38] S.O. Ganiyu, N. Oturan, S. Raffy, G. Esposito, E.D. van Hullebusch, M. Cretin, M.A. Oturan, Use of sub-stoichiometric titanium oxide as a ceramic electrode in anodic oxidation

and electro-Fenton degradation of the beta-blocker propranolol: Degradation kinetics and mineralization pathway, Electrochimica Acta. 242 (2017) 344–354.

[39] J. Zhao, J. Chen, S. Xu, M. Shao, D. Yan, M. Wei, D.G. Evans, X. Duan, CoMn-layered double hydroxide nanowalls supported on carbon fibers for high-performance flexible energy storage devices, J. Mater. Chem. A. 1 (2013) 8836.

[40] X. Cai, X. Shen, L. Ma, Z. Ji, C. Xu, A. Yuan, Solvothermal synthesis of NiCo-layered double hydroxide nanosheets decorated on RGO sheets for high performance supercapacitor, Chem. Eng. J. 268 (2015) 251–259.

[41] Y. Han, Z.-H. Liu, Z. Yang, Z. Wang, X. Tang, T. Wang, L. Fan, K. Ooi, Preparation of Ni^{2+} $-Fe^{3+}$layered double hydroxide material with high crystallinity and well-defined hexagonal shapes, Chem. Mater. 20 (2008) 360–363.

[42] M. Griffing, M.G. Mellon, Colorimetric determination of iron with various dioximes, Anal. Chem. 19 (1947) 1017–1020.

[43] S.O. Ganiyu, N. Oturan, S. Raffy, M. Cretin, R. Esmilaire, E. van Hullebusch, G. Esposito, M.A. Oturan, Sub-stoichiometric titanium oxide (Ti_4O_7) as a suitable ceramic anode for electrooxidation of organic pollutants: A case study of kinetics, mineralization and toxicity assessment of amoxicillin, Water Res. 106 (2016) 171–182.

[44] T.X.H. Le, T.V. Nguyen, Z. Amadou Yacouba, L. Zoungrana, F. Avril, D.L. Nguyen, E. Petit, J. Mendret, V. Bonniol, M. Bechelany, S. Lacour, G. Lesage, M. Cretin, Correlation between degradation pathway and toxicity of acetaminophen and its by-products by using the electro-Fenton process in aqueous media, Chemosphere. 172 (2017) 1–9.

[45] G. Nagaraju, G.S.R. Raju, Y.H. Ko, J.S. Yu, Hierarchical Ni–Co layered double hydroxide nanosheets entrapped on conductive textile fibers: a cost-effective and flexible electrode for high-performance pseudocapacitors, Nanoscale. 8 (2016) 812–825.

[46] Q. Wang, S. Tian, J. Long, P. Ning, Use of Fe(II)Fe(III)-LDHs prepared by co-precipitation method in a heterogeneous-Fenton process for degradation of Methylene Blue, Catal. Today. 224 (2014) 41–48.

[47] X. Long, Z. Wang, S. Xiao, Y. An, S. Yang, Transition metal based layered double hydroxides tailored for energy conversion and storage, Mater. Today. 19 (2016) 213 - 226.

[48] Y. Li, L. Zhang, X. Xiang, D. Yan, F. Li, Engineering of ZnCo-layered double hydroxide nanowalls toward high-efficiency electrochemical water oxidation, J. Mater. Chem. A. 2 (2014) 13250.

[49] T.X.H. Le, M. Bechelany, S. Lacour, N. Oturan, M.A. Oturan, M. Cretin, High removal efficiency of dye pollutants by electron-Fenton process using a graphene based cathode, Carbon. 94 (2015) 1003–1011.

[50] P. Geng, J. Su, C. Miles, C. Comninellis, G. Chen, Highly-ordered Magnéli Ti_4O_7 nanotube arrays as effective anodic material foreElectro-oxidation, Electrochimica Acta. 153 (2015) 316–324.

[51] D. Bejan, J.D. Malcolm, L. Morrison, N.J. Bunce, Mechanistic investigation of the conductive ceramic Ebonex® as an anode material, Electrochimica Acta. 54 (2009) 5548–5556.

[52] N. Oturan, J. Wu, H. Zhang, V.K. Sharma, M.A. Oturan, Electrocatalytic destruction of the antibiotic tetracycline in aqueous medium by electrochemical advanced oxidation processes: Effect of electrode materials, Appl. Catal. B Environ. 140–141 (2013) 92–97.

[53] A. Dirany, I. Sirés, N. Oturan, A. Özcan, M.A. Oturan, Electrochemical treatment of the antibiotic sulfachloropyridazine: Kinetics, reaction pathways, and toxicity evolution, Environ. Sci. Technol. 46 (2012) 4074–4082.

[54] E. Brillas, S. Garcia-Segura, M. Skoumal, C. Arias, Electrochemical incineration of diclofenac in neutral aqueous medium by anodic oxidation using Pt and boron-doped diamond anodes, Chemosphere. 79 (2010) 605–612.

[55] A. Özcan, Y. Şahin, A.S. Koparal, M.A. Oturan, A comparative study on the efficiency of electro-Fenton process in the removal of propham from water, Appl. Catal. B Environ. 89 (2009) 620–626.

[56] M.A. Oturan, M. Pimentel, N. Oturan, I. Sirés, Reaction sequence for the mineralization of the short-chain carboxylic acids usually formed upon cleavage of aromatics during electrochemical Fenton treatment, Electrochimica Acta. 54 (2008) 173–182.

[57] S. Garcia-Segura, E. Brillas, Mineralization of the recalcitrant oxalic and oxamic acids by electrochemical advanced oxidation processes using a boron-doped diamond anode, Water Res. 45 (2011) 2975–2984.

[58] S.H. Li, D. Bejan, M.S. Mcdowell, N.J. Bunce, Mixed first and zero order kinetics in the electrooxidation of sulfamethoxazole at a boron-doped diamond (BDD) anode, J. Appl. Electrochem. 38 (2008) 151–159.

[59] A. Dirany, S. Efremova Aaron, N. Oturan, I. Sirés, M.A. Oturan, J.J. Aaron, Study of the toxicity of sulfamethoxazole and its degradation products in water by a bioluminescence method during application of the electro-Fenton treatment, Anal. Bioanal. Chem. 400 (2010) 353–360.